



## **Structural Design and Hydrodynamic Force Analysis of Submersible Pressure Hull**

**Lella Swarana Mukhi**

*Research Scholar,*

*Jawaharlal Nehru Technological University Kakinada  
University College of Engineering  
Vizianagaram, (O.R.) [INDIA]  
Email: [swarnadas111@gmail.com](mailto:swarnadas111@gmail.com)*

**K. Srinivasa Prasad**

*Assistant Professor,*

*Department of Mechanical Engineering  
Jawaharlal Nehru Technological University Kakinada  
University College of Engineering  
Vizianagaram, (O.R.) [INDIA]  
Email: [ksprasad.me@jntukucev.ac.in](mailto:ksprasad.me@jntukucev.ac.in)*

### **ABSTRACT**

*Submersibles are more ubiquitous in their role in oceanographic research in the deep ocean. Extensive use of Marine Remotely Operating Vehicle (MROV's) in oceanographic applications necessitates investigation of hydrodynamic forces acting over an MROV hull form operating under deeply submerged condition. Hydrodynamic Force coefficients strongly affect the dynamic performance of autonomous underwater vehicle. The geometrical parameters needed for designing MROV are obtained from an existing underwater vehicle available in the literature (Myring hull profile). Estimation of hydrodynamic force coefficients (lift, drag, moment) were carried out at typical speed of 5.6m/s at varying angle of attack/pitching angles ( $0^{\circ}$ - $8^{\circ}$ ) using slender body theory and computational fluid dynamics using ANSYS 181.CFX approach (ANSYS) allows for a good prediction of the coefficients over the range of angles of attack considered.*

*Acceleration Hydrodynamic coefficients of the Submersible pressure hull are estimated by using Strip theory and Lamb inertia theory are found to be in good agreement. The pressure hull is subjected to repeated compressive stresses due to varying external hydraulic pressure and hence knowledge of various stresses acting on the structure and also the*

*buckling phenomena existing due to surrounding hydrostatic pressure is essential for designing the pressure hull. Static stresses on the pressure hull when subjected to External hydrostatic pressure were computed by using ANSYS workbench software. The Equivalent Von-mises stress is found to be less than the allowable strength of the Aluminium alloy material considered. Maximum deformation was considered safe. Buckling factor for the pressure hull was 9.5 with 10Mpa external pressure, which is considered very safe from design considerations.*

**Keywords:**— MROV, Slender body theory, strip theory, Lamb inertia theory, CFX, ANSYS, Lift, Drag, Moment.

### **I. INTRODUCTION**

Small unmanned submersibles called “Marine Remotely Operating Vehicles” (MROVs) are widely used today to work in water too deep or too dangerous for divers. MROVs repair offshore oil platforms and attach cables to sunken ships to hoist them. Such MROVs are attached by tether (a thick cable providing power and communication) to a control center on a ship. Operators on the ship see video images sent back from the robot and may control its propellers and manipulator arm. The wreck of the titanic was explored by

such a vehicle, as well as by a manned vessel. MROV is a camera mounted in a waterproof enclosure, with thrusters for manoeuvring, attached to a cable to the surface over which a video signal is transmitted. Today underwater vehicles are becoming more popular especially for environmental monitoring and for defense purposes. They are being widely used in commercial, scientific and military missions for explorations of water basin, temperature, and composition of the surrounding fluid, current speed, tidal waters and life forms in its natural habitats.

## II. DESIGN AND ANALYSIS

### *Hydrodynamic Force Coefficients*

**Computational Fluid Dynamics:** Computational Fluid Dynamics (CFD) is considered as the most competent means to calculate hydrodynamic forces of a marine vehicle. Comparatively, a CFD method is less costly and less time-consuming than an experimental method. However, CFD has readily become an effective tool that can attain a full set of hydrodynamic coefficients for marine vehicles. CFD is the analysis of systems involving flow, heat transfer and associated phenomenon such as chemical reactions by means computer-based simulations. It is the art of replacing the differential equations erring the fluid flow, with a set of algebraic equations, which in turn be solved with aid of digital computer to get an appropriate solution. The technique is very powerful spans a wide range of industrial and non-industrial application areas. CFD provides a good example of the many areas that a scientific computing project can touch on, and its relationship to computer science. Fluid flows are modeled by a set of PDE, the Navier-Stokes equation. On the discretized mesh, Navier-Stokes equation takes the form of large system of non-linear equations going from continuous to discrete

set of equations is a problem that combines both physics & numerical analysis.

The outer profile of the Submersible vehicle considered in the present study is streamlined to minimize the drag force and is having Length to Diameter ratio of 8.9. The CAD model is imported into ANSYS geometry module and the model is enclosed with the fluid domain and the whole assembly is divided into two half halves and meshing is carried out with proper refinement around the submersible pressure hull using inflation option to predict accurately the drag and lift forces. The meshed fluid domain along with the pressure hull body is presented in the following figures.

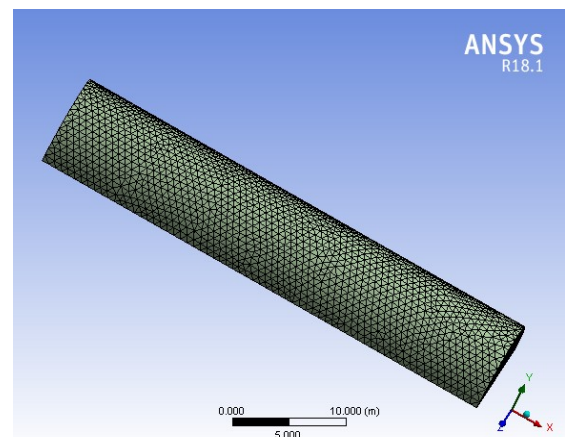


Figure 1: Meshed MROV

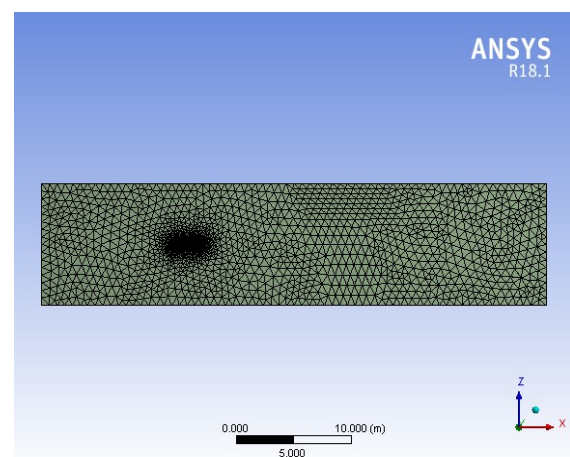


Figure 2: Meshed MROV

**Slender body theory:** The hydrodynamic Force coefficients  $C_l$ ,  $C_d$ ,  $C_m$  of MROV are computed and variations of these parameters wrt  $\alpha$ , angle of attack are presented.

**Acceleration Hydrodynamic coefficients**

**Strip theory:** The parent axisymmetric MROV hull form with maximum length,  $l$  and diameter,  $d$  can be divided into three regions, i.e., nose section, mid body section and the tail section. Nose section is hemi spherical, middle section is cylindrical in shape and tail section is elliptical in shape.

**Lamb inertia theory:** The next validation case considers a slightly more complicated object, a spheroid. Setting the same density of seawater, a test case can be performed on this Prolate spheroid to determine the added mass/inertia terms. This case is relevant since additional added inertia terms should show up in the solution, unlike the sphere case.

**III. RESULTS AND DISCUSSION:**

**Estimation of hydrodynamic Force coefficients**

The hydrodynamic Force coefficients of the MROV are estimated using slender body theory and Computational Fluid Dynamics software (ANSYS-workbench).

**Table 1: Hydrodynamic Force Coefficients Using CFX**

Angle of attack (deg)	Drag coefficient (Cd)	Lift coefficient (Cl)	Moment coefficient (Cm)	Drag force (Newtons)	Lift force (Newtons)
0	0.022	0.118	-7.6	66	334
2	0.024	0.106	-6.8	72	298
4	0.026	0.096	-6.32	76	272
6	0.028	0.090	-6.00	78	258
8	0.030	0.086	-6.00	82	254

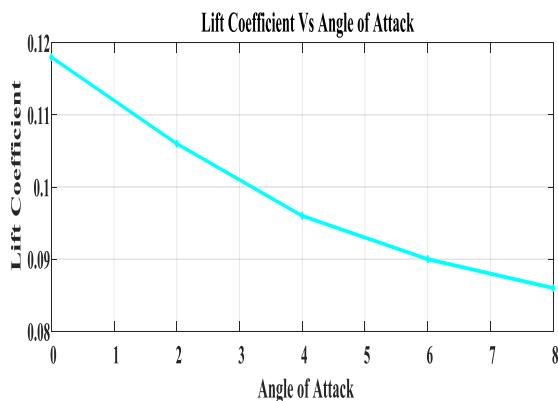


Figure 3: Coefficient of Lift of MROV Vs Angle of Attack  $\alpha$

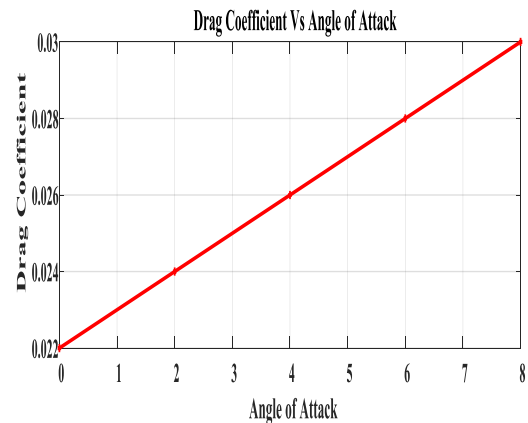


Figure 4: Coefficient of Drag of MROV Vs Angle of Attack  $\alpha$

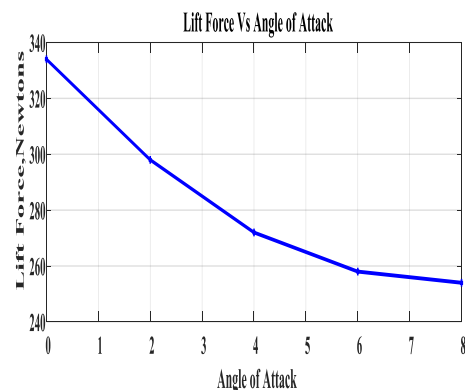


Figure 5: Lift force of MROV Vs Angle of Attack  $\alpha$

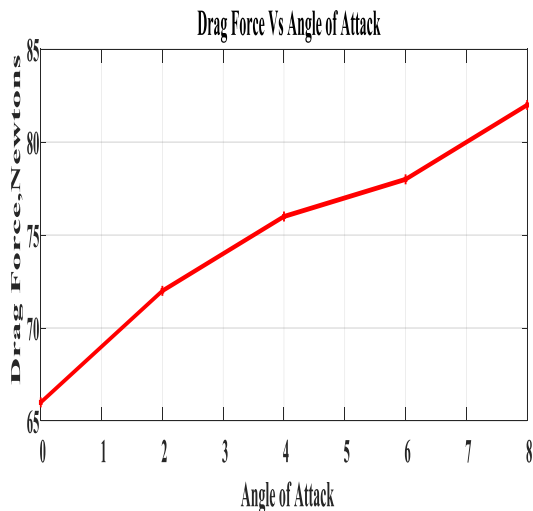


Figure 6: Drag force of MROV Vs Angle of Attack alpha

Referring to figures 2 & 5, it is observed that as the drag coefficient increases with increasing angle of attack while opposite trend is seen in case of lift coefficient. The body consider as axi-symmetric with no appendages and hence the pressure distribution around the body do not show much difference in value unlike as airfoil factors where the drag coefficient shown parabolic trend increase in value with increase in angle. It is above seen that even at zero angle the lift force is generated and also it has large value lift 334 Newtons compare to 66 Newtons drag force.

Table 2: Comparison of Slender Body Theory & CFX Values of Coefficient of Drag (CD) of MROV

Angle of attack	Slender body theory	CFX values
0	0.018	0.022
2	0.020	0.024
4	0.023	0.026
6	0.026	0.028
8	0.032	0.030

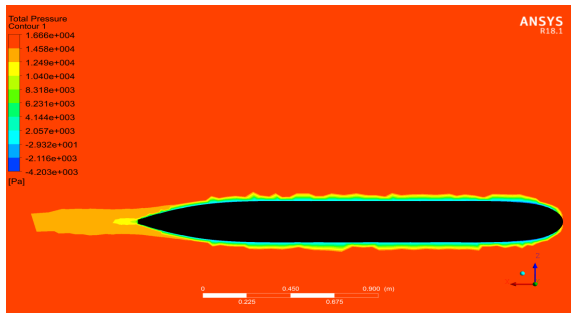
Table 3: Comparison of Slender Body Theory & CFX Values of Coefficient of Lift (CL) of MROV

Angle of attack	Slender body theory	CFX values
0	-7.4	-7.6
2	-6.5	-6.8
4	-6.23	-6.32
6	-6.03	-6.00
8	-5.57	-6.00

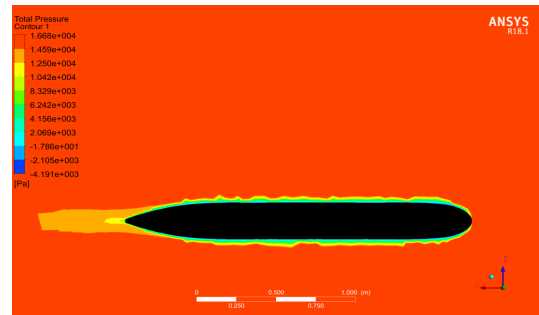
Table 4: Comparison of Slender Body Theory & CFX Values of Coefficient of Lift (CL) of MROV

Angle of attack	Slender body theory	CFX values
0	0.116	0.118
2	0.106	0.106
4	0.094	0.096
6	0.091	0.090
8	0.093	0.086

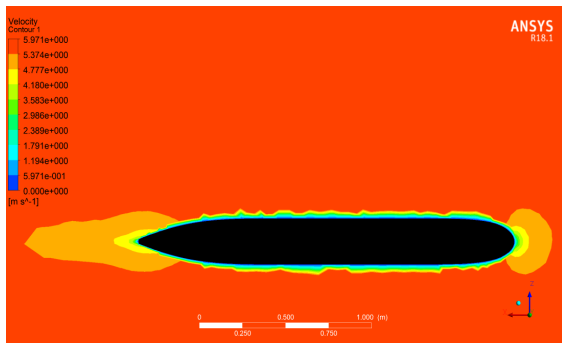
From the below contours of pressure and velocity at 0deg to 8deg we observe that the maximum total pressure developed due to the inlet velocity of 5.6 m/sec is 16680 Pascals in all cases of angles of attack. The reference pressure and relative pressure at outlet being set at zero Pascals. The maximum total pressure value of 16680 Pascals is hardly due to conversion of velocity head to pressure head. . The gradual increase in pressure away from submersible hull surface is due to frictional resistance offered by the hull (change in pressure indicated by green, yellow and red colors are seen from hull surface ).



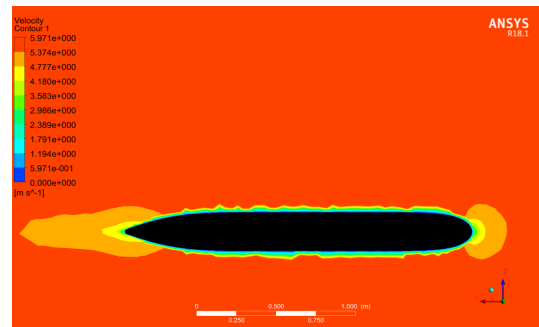
Contours of Pressure



Contours of Pressure



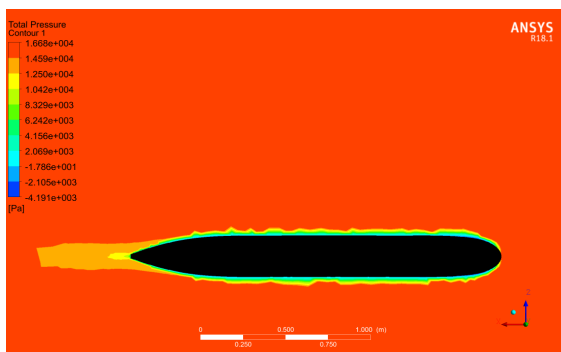
Contours of Velocity



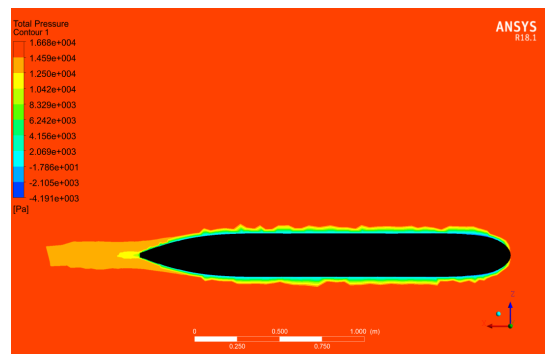
Contours of Velocity

Figure 7: Contours of Pressure and Velocity at 0deg

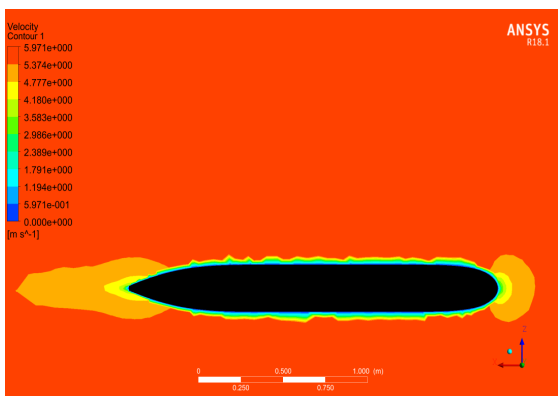
Figure 9: Contours of Pressure and Velocity at 4deg



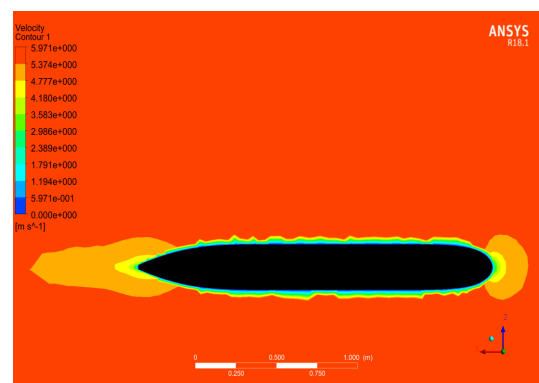
Contours of Pressure



Contours of Pressure



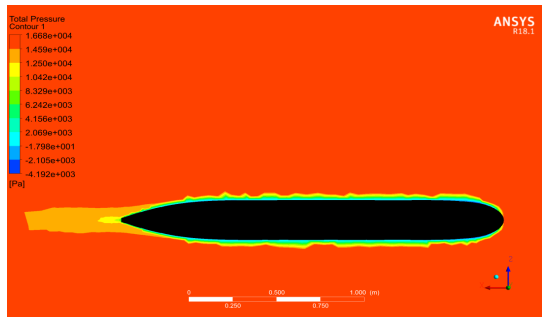
Contours of Velocity



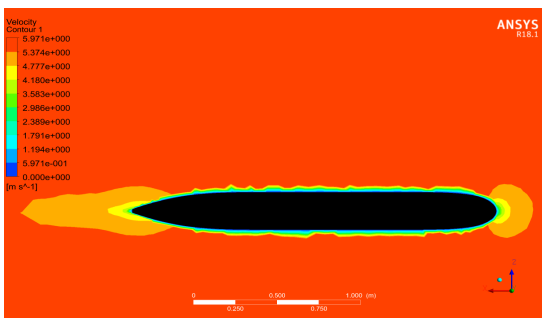
Contours of Velocity

Figure 8: Contours of Pressure and Velocity at 2deg

Figure 10: Contours of Pressure and Velocity at 6deg



Contours of Pressure



Contours of Velocity

Figure 11: Contours of Pressure and Velocity at 8deg

The mesh up around the hull has been taken care increasing a very fine mesh around the hull outer surface. The mesh gradually becomes coarser and coarser as the distance from surface increases. The fine mesh is redundant to capture the boundary layer surrounding the outer hull surface. The small yellow streak followed by large dark yellow streak is the total pressure contours at all angles shown gradually build up for pressure as the distance of the tail surface. The velocity contour plots at all angles of the attack shown same trend. The gradual decrease in velocity as the fluid approaches the nose is clearly seen in the contours. However the length of the yellow streak is more pronounced at the tail end than at the front nose end. Which could be due to the gradual change in cross section of the tail portion. Similar changes in colors as observed the pressure contours around the hull surface is also observed for the velocity contours showing gradual increase in velocity as the distance from hull surface increases.

**Acceleration Hydrodynamic coefficients :**

**Table 5 Axial added mass coefficients**

Parameter	Value	Units
$x_{udot}$	-1.5955	kg/m

**Table 6: Rolling Added Mass Coefficients**

Parameter	Value	Units
$k_{pdot}$	0	kg/m

**Table 7: Cross Flow Added Mass Coefficients**

Parameter	Strip theory	Lamb's Inertia Theory	Units
$X_{udot}$	-1.2346	-1.5955	kg
$Y_{vdot}$	-51.6289	-55.8889	kg
$Z_{wdot}$	-51.6289	-55.8889	kg
$M_{qdot}$	-8.7146	-8.1329	Kg.m <sup>2</sup> /rad
$N_{rdot}$	-8.7146	-8.1329	Kg.m <sup>2</sup> /rad

The Cross flow added mass coefficients of MROV is calculated using strip theory on both cylindrical and cruciform hull cross sections represented in table. The cross flow added mass coefficients are obtained by these characteristic parameters represented in Equations.. The differences obtained by calculating acceleration cross flow added mass coefficients using strip theory were shown in table. The Cross Flow added mass coefficients using lambs Inertia Theory are determined and the coefficients values were compared with the values obtained using strip theory. Cross flow added mass coefficients were shown in Equations.

### Static structural Analysis of MROV Pressure hull

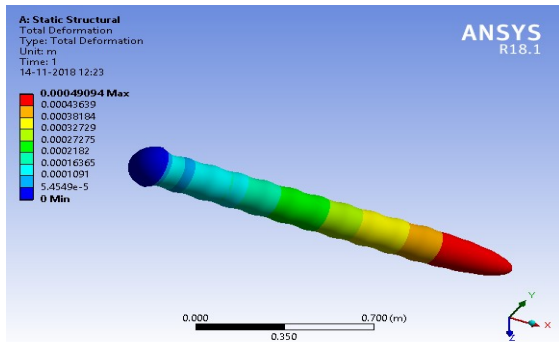


Figure 12: Total Deformation of MROV Pressure hull

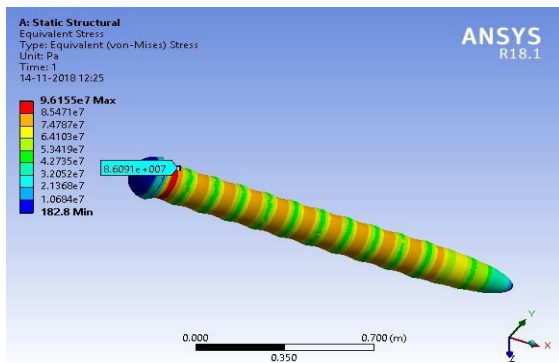


Figure 13: Equivalent Stress

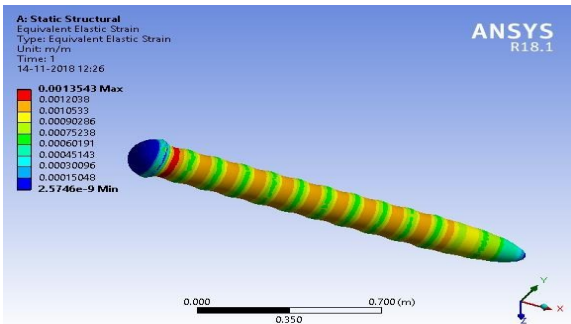


Figure 14: Elastic Strain

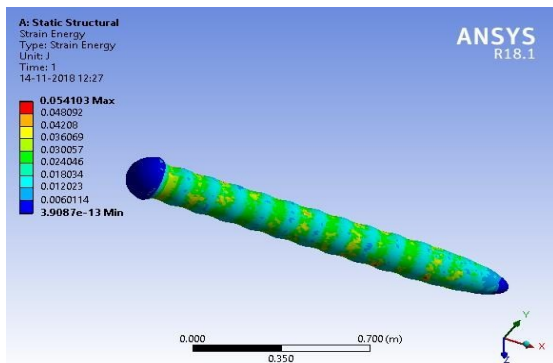


Figure 15: Strain Energy

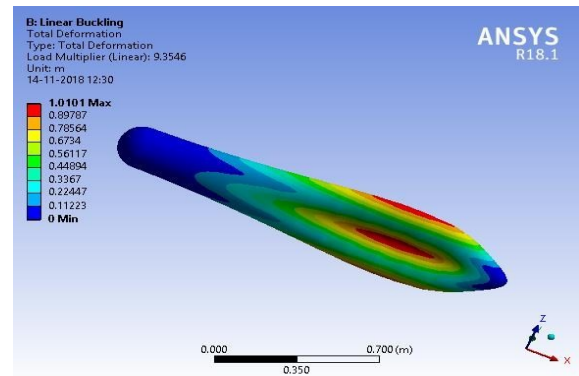


Figure 16 Linear Buckling-Total Deformation

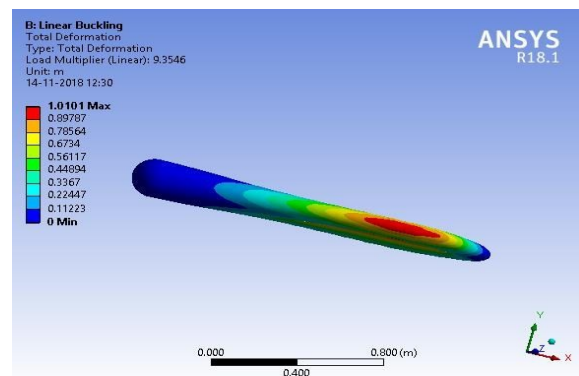


Figure 17: Linear Buckling-Total Deformation (side view)

Static stresses on the pressure hull when subjected to 10Mpa External hydrostatic pressures were computed by using ANSYS structural software. Maximum Von mises stress was 86Mpa which is much below than allowable stress of the aluminum alloy Material (240Mpa -0.2% proof strength). Maximum deformation was 0.5 which is considered safe. Buckling factor for the pressure hull was 9.5 with 10Mpa External pressures which is considered very safe from design considerations. Normally the structures are designed only for a factor of safety maximum 2 and not more than 3. So the structure is considered over designed and it is seen from buckling figures. The failure has taken over a number of ribs and not between 2 or 3 ribs. The failure is considered to be general instability and not interference buckling because the failure is spread over a number of ribs. Inter frame instability only occur in 2 ribs. In this case

general instability at a pressure of 95Mpa i.e.,  $9.5 \times 10$ Mpa applied pressure. The general stability will only occur at 95Mpa.

Hence from the structural design point of view shell is considered safe in yield criteria. Inter frame buckling and overall instability.

**REFERENCES:**

- [1] Allen and Edward Perkin “A Study of viscosity on flow over slender inclined bodies of revolution”
- [2] M. M. Karim, M. M. Rahman and M. A. Alim “Computation of Turbulent Viscous Flow around Submarine Hull Using Unstructured Grid”
- [3] P.Jagadeesh, K.Murali, V.G.Idichandy “Experimental investigation of hydrodynamic force coefficients over MROV hull.
- [4] Investigation of Normal Force and Moment Coefficients for an AUV at Nonlinear Angle of Attack and Sideslip Range.
- [5] Timothy Prester “Verification of a Six-Degree of Freedom Simulation Model for the REMUS Autonomous Underwater Vehicle”
- [6] Chiok Ching Chaw, “Modeling and Control of An Submersible”, *Master’s thesis, NUS, Department of Mechanical and Production Engineering*, 2000
- [7] K.R. Goheen, “Modeling Methods for Underwater Robotic Vehicle Dynamics”, *Journal of Robotic Systems*, vol. 8, no.3, pp. 259-317, 1991.

\* \* \* \* \*